

RESEARCH ARTICLE

Reduction of Proliferation and Induction of Apoptosis are Associated with Shrinkage of Head and Neck Squamous Cell Carcinoma due to Neoadjuvant Chemotherapy

Shreya Sarkar¹, Guru Prasad Maiti¹, Jayesh Jha², Jaydip Biswas², Anup Roy³, Susanta Roychoudhury⁴, Tyson Sharp⁵, Chinmay Kumar Panda^{1*}

Abstract

Background: Neoadjuvant chemotherapy (NACT) is a treatment modality whereby chemotherapy is used as the initial treatment of HNSCC in patients presenting with advanced cancer that cannot be treated by other means. It leads to shrinkage of tumours to an operable size without significant compromise to essential oro-facial organs of the patients. The molecular mechanisms behind shrinkage due to NACT is not well elucidated. **Materials and Methods:** Eleven pairs of primary HNSCCs and adjacent normal epithelium, before and after chemotherapy were screened for cell proliferation and apoptosis. This was followed by immunohistochemical analysis of some cell cycle (LIMD1, RBSP3, CDC25A, CCND1, cMYC, RB, pRB), DNA repair (MLH1, p53) and apoptosis (BAX, BCL2) associated proteins in the same set of samples. **Results:** Significant decrease in proliferation index and increase in apoptotic index was observed in post-therapy tumours compared to pre-therapy. Increase in the RB/pRB ratio, along with higher expression of RBSP3 and LIMD1 and lower expression of cMYC were observed in post-therapy tumours, while CCND1 and CDC25A remained unchanged. While MLH1 remained unchanged, p53 showed higher expression in post-therapy tumors, indicating inhibition of cell proliferation and induction of apoptosis. Increase in the BAX/BCL2 ratio was observed in post-therapy tumours, indicating up-regulation of apoptosis in response to therapy. **Conclusions:** Thus, modulation of the G1/S cell cycle regulatory proteins and apoptosis associated proteins might play an important role in tumour shrinkage due to NACT.

Keywords: Proliferation - apoptosis - neoadjuvant chemotherapy - head and neck squamous cell carcinoma

Asian Pac J Cancer Prev, 14 (11), 6419-6425

Introduction

Head and neck squamous cell carcinoma (HNSCC) is a major form of cancer in the Indian subcontinent, accounting for about 30-40% of all cancer types (Tripathi et al., 2003). Globally, it is the sixth most common cancer and ranks eighth in global cancer deaths (Shibuya et al., 2002), the global mortality rate being 6/100,000. The etiological factors include tobacco, betel nut and leaf quid, alcohol and HPV 16/18 infection (Koch et al., 1999).

Surgery is the most preferred and effective mode of treatment of HNSCC. For early lesions, surgery or radiation is recommended, whereas for advanced cases, surgery is recommended. However, only 10-15% of the patients present with early, localized disease, where a single modality of treatment is effective for cure (Sankaranarayanan, 1990). The majority of the cancers present late. Surgery in advanced HNSCC is often difficult, especially in India, due to lack of sufficient resources or expertise to cater to the needs for an overwhelming number

of patients. In recent years, induction chemotherapy, also called neoadjuvant chemotherapy (NACT), followed by surgery is the choice of treatment for patients presenting with locally advanced, unresectable disease. The main aim is to reduce the tumor volume to an operable size before surgery and also to enable maximum preservation of oro-facial organs. However, the mechanism of tumor volume reduction is not well understood.

In HNSCC, differential gradation of tumors were evident from the proximal to the distal sites, i.e., less differentiated cells were more prevalent at the core of the tumor, whereas more differentiated cells were seen at the periphery (Slaughter et al., 1953). It seems that these differentiated tumor cells were affected more due to neoadjuvant chemotherapy.

In HNSCC tumor progression model, it was evident that inactivation of LIMD1 (associated with RB/E2F interaction) occurred in chronic ulcerative stage, followed by inactivation of RBSP3 (associated with dephosphorylation of RB at serine 807/811) in mild

¹Department of Oncogene Regulation, ²Department of Surgical Oncology, Chittaranjan National Cancer Institute, ⁴Molecular and Human Genetics Division, Indian Institute of Chemical Biology, Kolkata, ³North Bengal Medical College and Hospital, West Bengal, India, ⁵Molecular Oncology, Barts Cancer Institute, London, United Kingdom *For correspondence: ckpanda.nci@gmail.com

dysplastic stage. In addition, inactivation of CDC25A occurred at moderate dysplastic stage, followed by activation of CCND1 and cMYC in the later stages of tumor development (Sabbir et al., 2006; Ghosh et al., 2008; 2010a; 2010b; Bhattacharya et al., 2009). As a result, there was hyperphosphorylation of RB for progression of the cell cycle. On the other hand, inactivation of MLH1, a DNA repair protein and p53 occurred at mild dysplastic stage, indicating the impairment of DNA repair as an early event in the development of the tumor (Maiti et al., 2012). Bcl2, an anti-apoptotic protein, shows decrease in expression from mild dysplasia (Loro et al., 2002).

Thus to understand the molecular mechanism of tumor shrinkage in HNSCC due to NACT, we wanted to analyze the alterations of these genes in tumors before and after chemotherapy. For this reason, firstly we have analyzed proliferation and apoptosis in 11 pairs of pre- and post-therapy HNSCC tumors from the same patients, along with their respective adjacent normal tissues. Secondly, immunohistochemical analysis of the cell cycle regulatory, DNA repair and apoptosis associated genes were done in the same samples. Our data suggests that inhibition of cellular proliferation and induction of apoptosis might be the reason for tumor shrinkage.

Materials and Methods

Patient population and tumor tissues

Eleven (11) pairs of primary HNSCC and adjacent normal epithelium were collected from the same patients, both before and after neoadjuvant chemotherapy from the hospital section of Chittaranjan National Cancer Institute, Kolkata, India. All patients received 3 cycles of chemotherapy with Cisplatin and 5-Fluorouracil in doses of 70-100 mg/m² and 1000 mg/m² B.S. A. respectively. Informed consent was obtained from the patients, as well as the hospital authorities and the institutional ethical committee had approved the study. All specimens, freshly obtained from punch biopsies or operated specimens, were fixed in 10% formalin for further work. All tumors were staged according to UICC TNM classification (Harmer, 1978). Tumor sites included cheek (n=4), lip (n=2), buccal mucosa (n=4) and alveolus (n=1) (Table 1).

Histopathological evaluation

Paraffin blocks, prepared from the formalin fixed tissue

samples, were sectioned at 3-4 μ m and hematoxylin-eosin (HE) staining carried out. Stained slides were visualized under a light microscope and photographed, followed by grading of the tumors by two independent certified pathologists.

Determination of expression of proteins by Immunohistochemical analysis

Immunohistochemical analysis was performed by HRP method according to standard procedures (Ghosh et al., 2010). In brief, 4-5 μ m paraffin sections were de-paraffinized in xylene, hydrated with decreasing grades of alcohol and finally PBS, antigen retrieved by heating in Citrate Buffer, pH 7.4 for 20 mins at 85°C and blocked with 3% BSA for 30 mins. Primary antibodies, used overnight in dilutions of 1:75 or 1:100 were LIMD1 (Rabbit polyclonal, CP-30-09) and RBSP3 (Rabbit polyclonal, CP-57-09) from Imgenix India Pvt. Ltd and CDC25A (Goat polyclonal IgG, sc-6947), MLH1 (Rabbit polyclonal IgG, sc-581), CCND1 (Mouse monoclonal IgG1, sc-246), cMYC (Mouse monoclonal IgG1, sc-40), RB (Rabbit polyclonal IgG, sc-7905), pRB (Rabbit polyclonal IgG, ser 807/811, sc-16670-R) and PCNA (Mouse monoclonal IgG 2a) from Santacruz Biotechnology. HRP-conjugated secondary antibodies, used in dilutions of 1:500 were rabbit anti-goat IgG (sc-2768), goat anti-rabbit IgG (sc-2004) and goat anti-mouse IgG (sc-2005) were also purchased from Santacruz Biotechnology, USA. 3, 3'-diaminobenzidine (DAB) was used to develop the slides and hematoxylin was used as the counter stain. Scoring of slides was done by two independent observers, calculating the average of the percentage of immunopositive cells in 4 randomly chosen fields. For the scoring of the adjacent normal epithelium, expression in the basal layer was considered, both for the nucleus, as well as for the cytoplasm independently. Considering that the basal layer of the normal epithelium is the proliferation zone, expression in the tumors, both pre- and post-chemotherapy was compared to the expression in the basal layer in the corresponding normal specimens, pre- and post-chemotherapy respectively. Images were obtained by using a bright field microscope (Leica EC 3, Germany).

Determination of apoptosis by TUNEL assay

In situ apoptosis was determined by the Terminal

Table 1. Clinicopathological Features of Head and Neck Lesions

REGN. NO.	A/S	SITE	TOBACCO	STAGE	GRADE	RESPONSE (CT)	HPV 16
32	50/Male	L BM	Present	III	I	GOOD	Present
2098	38/Female	L CHK	Present	III	I	GOOD	Absent
2548	40/Male	L CHK	Present	III	I	GOOD	Present
3953	40/Male	R BM	Present	III	I	MODERATE	Present
3992	60/Female	L BM, ALV, RMT	Present	III	I	GOOD	Present
184	52/Male	L BM	Present	III	II	GOOD	Present
397	50/Male	R CHK	Present	III	II	GOOD	Present
3873	60/Male	LIP	Present	III	II	GOOD	Present
4108	35/Male	LOW LIP	Present	IV	II	NEGATIVE	Present
2598	52/Male	L CHK	Present	III	III	GOOD	Present
1485	40/Male	ALV	Present	IV	III	GOOD	Present

*ALV: Alveolus, BM: Buccal mucosa, CHK: Cheek, RMT: Retromolar trigone

deoxynucleotidyl transferase (TdT) associated dUTP Nick End Labeling (TUNEL) Assay, utilizing a commercial in situ cell death detection peroxidase (POD) kit (Roche Molecular Biochemicals, Mannheim, Germany). Following the manufacturer's protocol, 4-5 μ m paraffin sections were initially deparaffinized and hydrated serially in xylene, descending grades of alcohol and PBS, permeabilized with 20 μ g/ml Proteinase K for 30 mins at 37°C and incubated with TUNEL reaction mixture for 60 mins at 37°C in a humidified chamber. The slides were washed with PBS and finally incubated with horseradish POD conjugated anti-fluorescein antibody and DAB as the chromogen for 30 mins at 37°C under humidified conditions. Stained slides were visualized and photographed under a bright field microscope (Manna et al., 2006).

Detection of HPV 16

HPV 16 was detected by immunohistochemical analysis of pre-treated tumors with HPV 16 E6 (goat polyclonal IgG, sc1584) antibody from Santacruz Biotechnology, USA according to the procedure stated above.

Statistical analysis

Results obtained were analyzed by Analysis of variance (ANOVA), followed by Tukey's Test, with the

help of Critical Difference (CD) or Least Significant Difference (LSD) at 5% (CD5) and 1% (CD1) level of significance. p values <0.05 and <0.01 were considered significant.

Results

Analysis of proliferation and apoptosis in tumors

The normal basal epithelium adjacent to the pre-therapy tumors showed high proliferative index (mean 92.92, SD \pm 3.27), which did not change significantly in basal layer of post-therapy adjacent normal (mean 91.48, SD \pm 4.0). However, the proliferation index in tumors significantly decreased from pre-therapy (mean 62.84, SD \pm 20.96) to post-therapy (mean 32.76, SD \pm 20.81, p<0.05) with 8/11 post therapy tumors showing >1.5 fold reduction in proliferation (Figure 1, 2).

Apoptotic index in basal layer pre-therapy adjacent normal was low (mean 3.17, SD \pm 1.81) and did not change significantly post therapy (mean 5.34, SD \pm 2.43). Pre-therapy, tumors did not show significant increase in apoptotic index compared to adjacent normal (mean 7.31, SD \pm 3.27). However, there was significant increase in the same in tumors post therapy (mean 24.18, SD \pm 14.04, p<0.01) with 6/11 tumors showing 1.5 fold or greater increase in apoptotic index (Figure 1, 3).

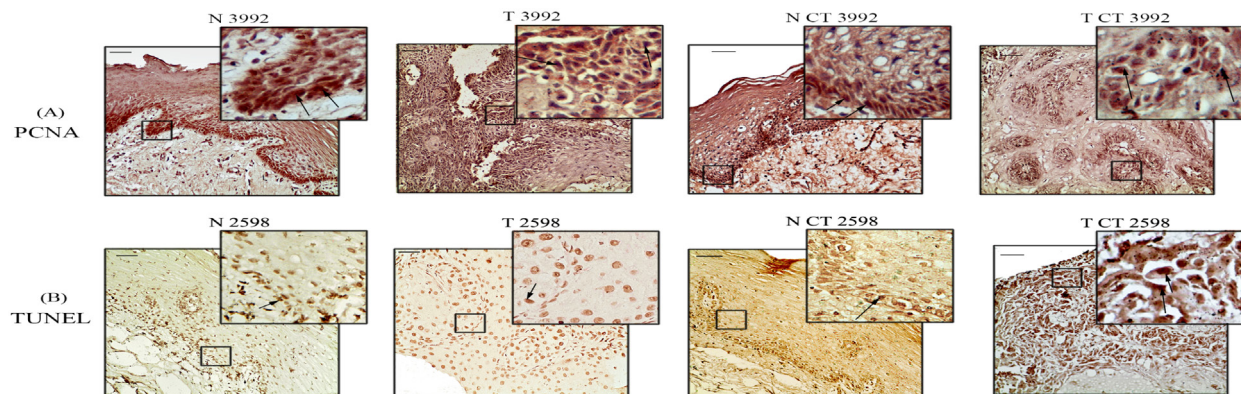


Figure 1. Immunohistochemical Analysis of (A) Proliferation Index and (B) Apoptotic Index. 3992, 2598 represent sample numbers. N: Adjacent normal, T: Tumor, NCT: Adjacent normal after NACT, TCT: Tumor after NACT. Black arrows indicate the expression and location of the markers. Magnification: 20X, Scale bar: 50 μ m

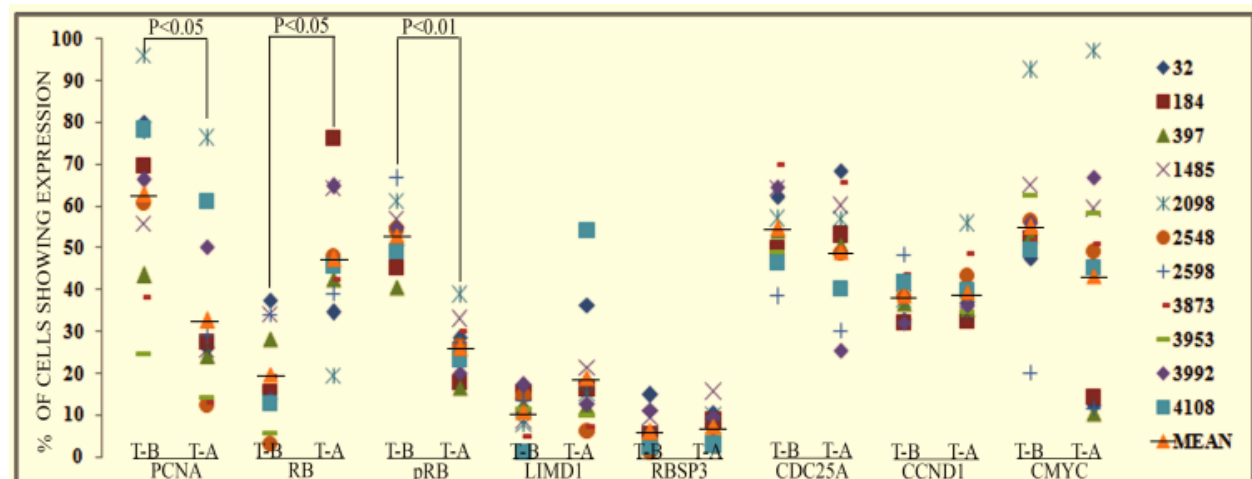


Figure 2. Graphical Representation of Proliferation Index and Percentage of cells Showing Nuclear Expression of Cell Cycle Associated Proteins in Tumors. T-B: Tumors before therapy, T-A: Tumors after therapy. Coloured symbols represent sample numbers. Yellow triangle represents mean of percentage of cells showing expression

Analysis of expression of cell cycle related proteins:

In basal epithelium of pre-therapy adjacent normal, RB showed moderate nuclear expression (mean 41.93, SD±17.36) whereas pRB showed nearly 2-fold high nuclear expression (mean 86.92, SD±7.63), with the pattern remaining similar post therapy (RB: mean 50.66, SD±15.38, pRB: mean 84.46, SD±7.25). This indicates that the high pRB expression is necessary for progression of cell cycle. Similarly, in pre-therapy tumors nearly 2.7-fold high expression of pRB (mean 53.03, SD±7.27) was

seen than RB expression (mean 19.69, SD±11.92). On the contrary, in post-therapy tumors, nearly 1.8-fold decrease in pRB expression (mean 26.09, SD±6.63) was seen than RB expression (mean 47.32, SD±15.83). This suggests that there is a restriction of G1/S cell cycle checkpoint in post-therapy tumors (Figure 2, 4).

In case of LIMD1, high nuclear expression in adjacent basal epithelium was seen in both pre (mean 96.94, SD±1.97) and post therapy (mean 89.72, SD±11.93). However, significant reduction of its expression was evident in tumors of both pre therapy (mean 10.7, SD±4.75) and post therapy (mean 19.04, SD±14.29), with >1.5-fold increase in expression in 5/11 post-therapy tumors (Figure 2, 7).

Interestingly, low expression of RBSP3 was seen in normal basal epithelium of both pre (mean 3.91, SD±1.55) and post (mean 3.88, SD±0.98) therapy, indicating high expression of pRB. Similar pattern of RBSP3 expression was also evident in pre-therapy tumors (mean 5.9, SD±4.18). However, in post-therapy tumors, comparatively high expression of RBSP3 was seen (mean 7.28, SD±3.99) with >1.5 fold higher expression 5/11 post-therapy tumors (Figure 2, 7).

CDC25A showed high nuclear expression in adjacent basal epithelium in both pre (mean 95.55, SD±3.82) and post therapy (mean 92.12, ±SD4.07) and moderate reduction in expression in tumors both pre (mean 54.73, SD±9.7) and post chemotherapy (mean 49.07, SD±13.85) (Figure 2, 7).

In the analysis of cell cycle activator CCND1, moderate

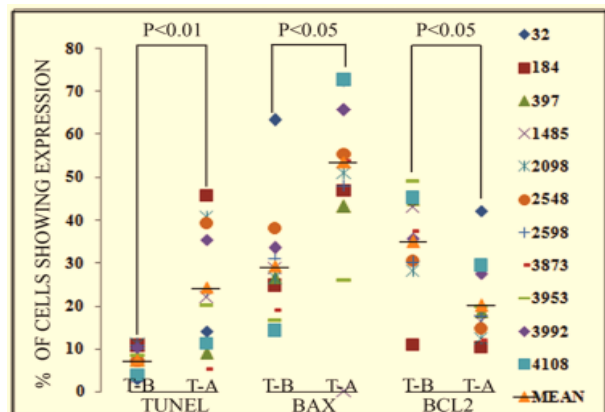


Figure 3. Graphical Representation of Apoptotic Index and Percentage of Cells Showing Cytoplasmic Expression of Apoptosis Associated Proteins in Tumors. T-B: Tumors before therapy, T-A: Tumors after therapy. Coloured symbols represent sample numbers. Yellow triangle represents mean of percentage of cells showing expression

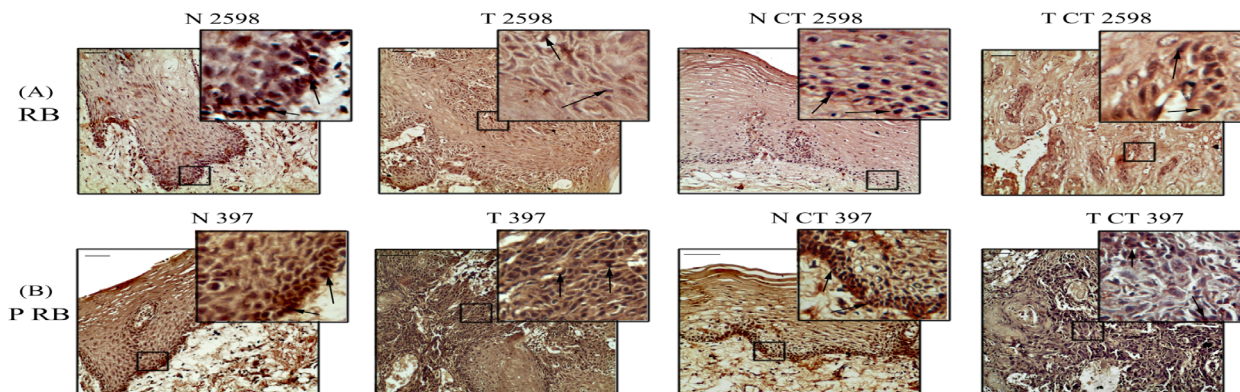


Figure 4. Immunohistochemical Expression of Cell Cycle Associated Proteins (A) RB and (B) pRB. 2598, 397 Represent Sample Numbers. N: Adjacent normal, T: Tumor, NCT: Adjacent normal after NACT, TCT: Tumor after NACT. Black arrows indicate the expression and location of the markers. Magnification: 20x, Scale bar: 50µm.

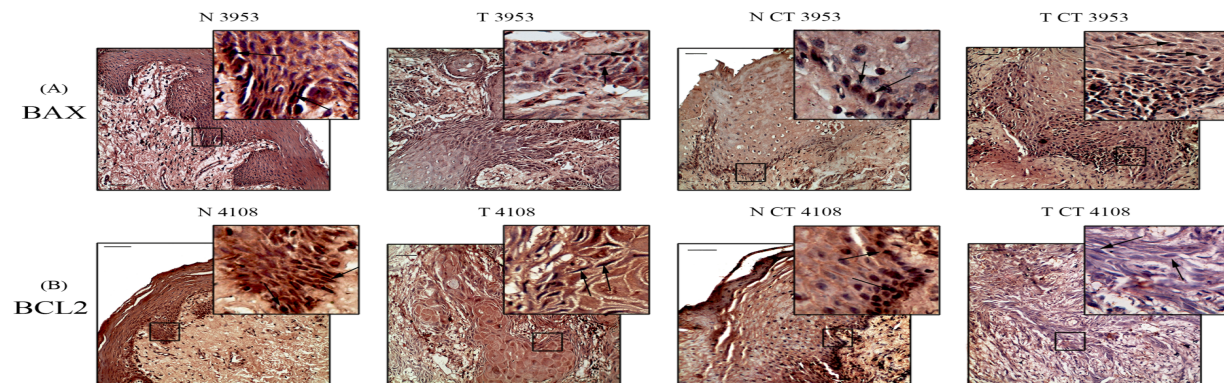


Figure 5. Immunohistochemical Expression of Apoptosis Associated Proteins (A) BAX and (B) BCL2. 3953, 4108 represent sample numbers. N: Adjacent normal, T: Tumor, NCT: Adjacent normal after NACT, TCT: Tumor after NACT. Black arrows indicate the expression and location of the markers. Magnification: 20x, Scale bar: 50µm

nuclear expression was seen in adjacent basal epithelium in both pre (mean 47.92, SD±11.79) and post therapy (mean 47.44, SD±9.35) with comparable expression of the same in tumors of both pre (mean 38.71, SD±5.17) and post therapy (mean 39.48, SD±7.14). Similarly, moderate expression of cMYC was seen in adjacent basal epithelium

of both pre (mean 45.52, SD±22.0) and post therapy (mean 45.09, SD±18.15), with the pattern remaining similar in tumors in both pre (mean 55.14, SD±17.03) and post (mean 43.21, SD±28.15) therapy, with >1.5 fold decrease in expression in 5/11 post therapy tumors (Figure 2, 7). This indicates that differential expression of cMYC and CCND1 expression occurs in post-therapy tumors.

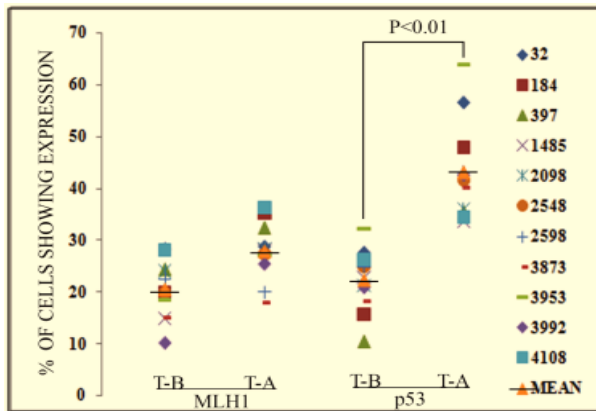


Figure 6. Graphical Representation of Nuclear Expression of DNA Damage Repair Associated Proteins in tumors. T-B: Tumors before therapy, T-A: Tumors after therapy. Coloured symbols represent sample numbers. Yellow triangle represents mean of percentage of cells showing expression

Study of apoptosis related proteins:

It was evident that the level of expression of BAX and BCL2 was comparable in normal basal epithelium in both pre (BAX: mean 79.3, SD±9.58, BCL2: mean 85.79, SD±7.97) and post therapy (BAX: mean 78.56, SD±8.46, BCL2: mean 89.86, SD±4.3). In pre-therapy tumors, expression of both the proteins was comparatively low (BAX: mean 29.28, SD±13.36, BCL2: mean 34.98, SD±10.77). However, in post therapy, BAX showed high cytoplasmic expression (mean 53.43, SD±14.26) compared to BCL2 (mean 20.02, SD±9.49) with 1.5-fold higher expression of BAX and BCL2 in 9/11 and 9/11 post therapy tumors respectively (Figure 3, 5).

Study of protein associated with DNA repair:

High nuclear expression MLH1 was seen in adjacent basal epithelium in both pre (mean 88.59, SD±20.82)

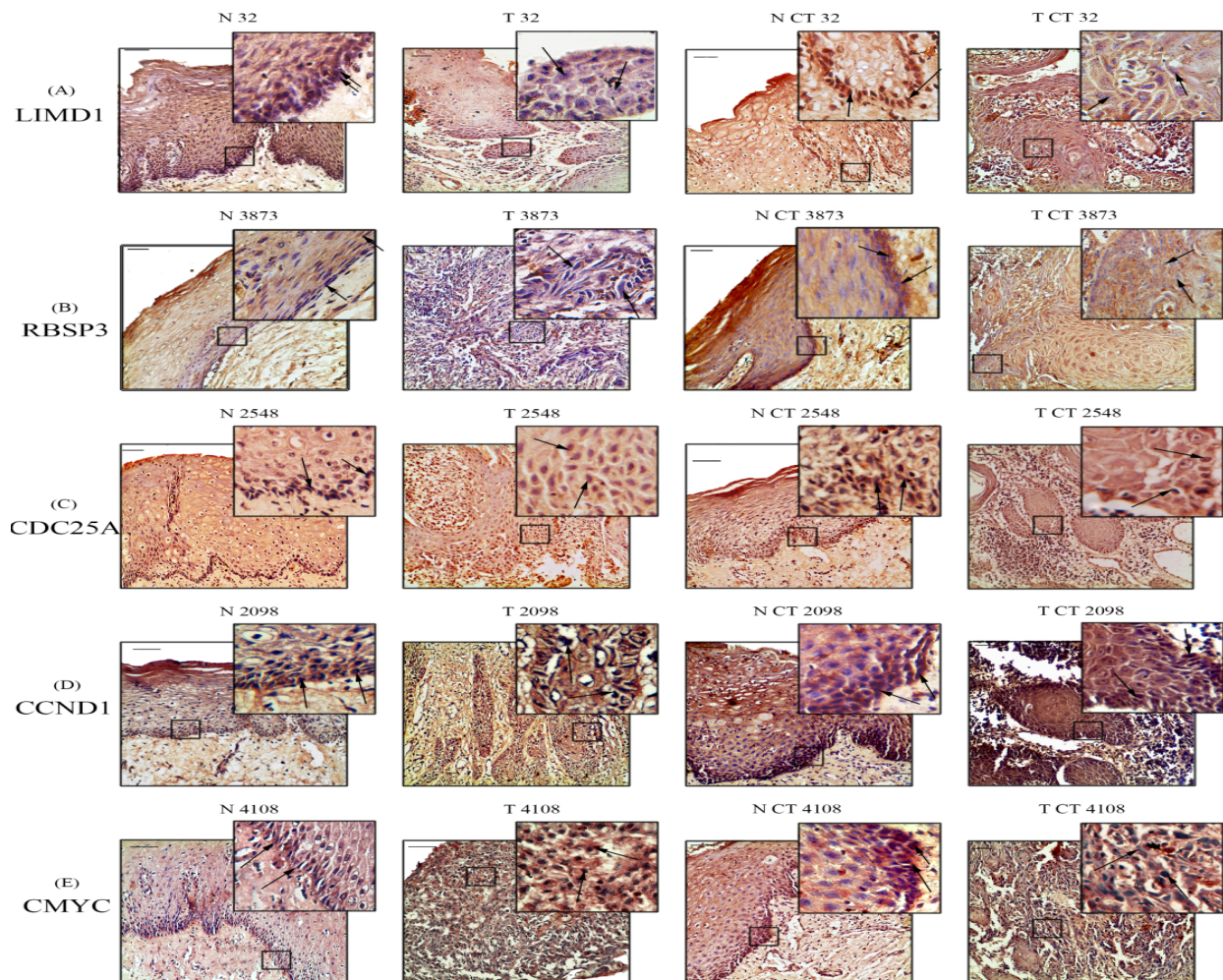


Figure 7. Immunohistochemical Expression of Cell Cycle Associated Proteins (A) LIMD1, (B) RBSP3, (C) CDC25A, (D) CCND1 and (E) cMYC. 32, 3873, 2548, 2098 and 4108 represent sample numbers. N: Adjacent normal, T: Tumor, NCT: Adjacent normal after NACT, TCT: Tumor after NACT. Black arrows indicate the expression and location of the markers. Magnification: 20X, Scale bar: 50µm.

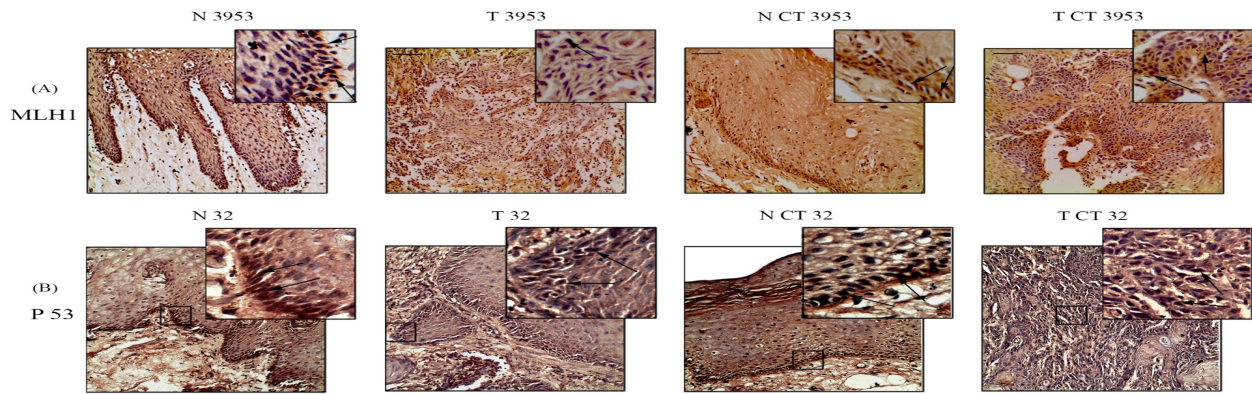


Figure 8. Immunohistochemical Expression of DNA Repair Associated Proteins (A) MLH1 and (B) p53. 3953, 32 Represent Sample Numbers. N: Adjacent normal, T: Tumor, NCT: Adjacent normal after NACT, TCT: Tumor after NACT. Black arrows indicate the expression and location of the markers. Magnification: 20X, Scale bar: 50µm.

and post therapy (mean 92.23, SD±2.13) with significant reduction in expression in tumors in both before (mean 20.82, SD±5.68) and after (mean 28.19, SD±5.62) therapy (Figure 6, 8). Similarly, high nuclear expression of p53 was evident in adjacent normal basal epithelium in both pre (mean 84.45, SD±8.0) and post therapy (mean 88.7, SD±9.15). However, increase in p53 expression was seen in post-therapy tumors (mean 43.39, SD±9.68) compared to pre-therapy (mean 22.64, SD±6.0) with >1.5-fold expression in 9/11 post therapy tumors (Figure 6, 8).

Discussion

In neoadjuvant chemotherapy using a combination of cisplatin and 5-fluorouracil as the first regimen, high response rates were obtained (Jacobs et al., 1987, Karp et al., 1991). In spite of the extensive use of this form of treatment in the current times, the molecular mechanism behind tumor shrinkage due to NACT remains elusive. Therefore, to decipher the mechanism of tumor shrinkage, our study focused on two main aspects-apoptosis and proliferation, perturbation of either or both of which may lead to decrease in tumor volume following therapy.

It was evident that in the tumors after neoadjuvant chemotherapy, there was significant decrease in proliferation index and increase in apoptotic index. To the best of our knowledge, similar kind of study was not reported in HNSCC. However Costa et al. (2001) showed that increase in apoptotic index and decrease in mitotic index and its associated markers in cervical cancer had a good prognosis after NACT. Similarly, in breast and gastric carcinomas, increase in apoptotic index was observed in post-therapy tumors (Tiezzi et al., 2006, Jia et al., 2012).

Significant increase in expression of RB and decrease in pRB was observed in majority of post-therapy tumors (6/11, 11/11 respectively) compared to pre-therapy. This shift in RB, pRB expression indicated a restriction of the cell cycle progression. This decrease in pRB expression might be due to the increase in RBSP3 expression in post therapy tumors than pre-therapy as concordance has been seen between RBSP3 and pRB expression. Similar pattern of expression was also seen for LIMD1, indicating an increase in RB-E2F interaction. Additionally, we have not seen any significant changes in expression pattern of

CCND1 in pre and post therapy tumors. This indicates that RBSP3 and LIMD1 might have synergistic effect in restriction of the cell cycle in post-therapy tumors, suggesting their prognostic importance. Similar data has not yet been reported. However, increase in RBSP3 and LIMD1 expression, along with down-regulation of pRB expression has been reported in chemoprevention of liver carcinogenesis in mouse by amarogentin (Pal et al., 2012). On the other hand, reduced expression of cMYC in some post-therapy tumors (5/11) indicates the importance of this gene in inhibition of cell proliferation.

The insignificant change in expression of MLH1 in post-therapy tumors compared to pre-therapy indicates that mismatch repair pathway might not be associated with response to NACT. On the other hand, up-regulation of p53 in post-therapy tumors (9/11) than pre-therapy suggests the importance of this gene in inhibition of cell proliferation and induction of apoptosis. Interestingly, concordance has been seen with HPV16 prevalence and p53 up-regulation in the tumors. It seems that in HPV positive tumors, at least one of the p53 alleles is in wild type state and its up-regulation might activate the G1/S checkpoint, along with induction of apoptosis of the differentiated cells, as evident from previous studies (Sultana et al., 2003; Mitra et al., 2007). This induction might be due to the up-regulation of BAX by p53, as concordance has been seen between expressions of these proteins in post-therapy tumors.

On the other hand, decrease in BCL2 expression in majority of the post-therapy tumors (9/11), resulting in increase in BAX/BCL2 ratio suggests the association of the intrinsic pathway of apoptosis in shrinkage of tumors. The association of BAX/BCL2 in response to NACT has been reported in different tumors including HNSCC (Matsumoto et al., 2004).

Thus, from the study, it can be concluded that the tumor shrinkage due to NACT is due to the synergistic effect of reduction of cell proliferation and induction of apoptosis. The restriction of cellular proliferation is mainly due to blockage of the G1/S cell cycle checkpoint by up-regulation of RB/pRB ratio and p53, and induction of apoptosis is due to increase in BAX/BCL2 ratio. However, more samples need to be analyzed in order to understand the detailed molecular mechanism of tumor shrinkage due to NACT.

Acknowledgements

The authors thank the Director of Chittaranjan National Cancer Institute, Kolkata, India, for his kind cooperation. Financial support for this work was provided by grants from Department of Biotechnology (BT/PR/5524/Med/14/649/2004), Government of India, to Dr CK Panda and Dr S Roychoudhury, Council of Scientific and Industrial Research-Project, New Delhi, India (IAP-001) to Dr. S. Roychoudhury, Council for Scientific and Industrial Research, Grant No. 09/030(0056)/2010 EMR-I to Shreya Sarkar. The authors also thank Dr. S. S. Mondal, Chittaranjan National Cancer Institute, Kolkata, for his kind cooperation in statistical analysis.

References

- Bhattacharya N, Roy A, Roy B, et al (2009). MYC gene amplification reveals clinical association with head and neck squamous cell carcinoma in Indian patients. *J Oral Pathol Med*, **38**, 759-63.
- Costa S, Terzano P, Santini D, et al (2001). Neoadjuvant chemotherapy in cervical carcinoma: regulators of cell cycle, apoptosis, and proliferation as determinants of response to therapy and disease outcome. *Am J Clin Pathol*, **116**, 729-37.
- Ghosh A, Ghosh S, Maiti GP, et al (2010). Frequent alterations of the candidate genes hMLH1, ITGA9 and RBSP3 in early dysplastic lesions of head and neck: clinical and prognostic significance. *Cancer Sci*, **101**, 1511-20.
- Ghosh S, Ghosh A, Maiti GP, et al (2010). LIMD1 is more frequently altered than RB1 in head and neck squamous cell carcinoma: clinical and prognostic implications. *Molecular cancer*, **9**, 58.
- Harmer MH (1978). UICC TNM classification of malignant tumors, 3rd edn. Geneva: Union Internationale Contre le Cancer (UICC).
- Jacobs C, Goffinet DR, Goffinet L, et al (1987). Chemotherapy as a substitute for surgery in the treatment advanced resectable head and neck cancer. A report from the Northern California Oncology Group. *Cancer*, **60**, 1178-83.
- Jia Y, Dong B, Tang L, et al (2012). Apoptosis index correlates with chemotherapy efficacy and predicts the survival of patients with gastric cancer. *Tumour Biol*, **33**, 1151-8.
- Karp DD, Vaughan CW, Carter R, et al (1991). Larynx preservation using induction chemotherapy plus radiation therapy as an alternative to laryngectomy in advanced head and neck cancer. A long-term follow-up report. *Am J Clin Oncol*, **14**, 273-9.
- Koch WM, Lango M, Sewell D, et al (1999). Head and neck cancer in nonsmokers: a distinct clinical and molecular entity. *The Laryngoscope*, **109**, 1544-51.
- Loro LL, Johannessen AC, Vintermyr OK (2002). Decreased expression of bcl-2 in moderate and severe oral epithelia dysplasias. *Oral oncol*, **38**, 691-8.
- Maiti GP, Ghosh A, Chatterjee R, et al (2012). Reduced expression of limd1 in ulcerative oral epithelium associated with tobacco and areca nut. *Asian Pac J Cancer Prev*, **13**, 4341-6.
- Manna S, Banerjee S, Mukherjee S, et al (2006) Epigallocatechin gallate induced apoptosis in Sarcoma180 cells in vivo: mediated by p53 pathway and inhibition in U1B, U4-U6 UsnRNAs expression. *Apoptosis*, **11**, 2267-76.
- Mathers CD, Shibuya K, Boschi-Pinto C, et al (2002). Global and regional estimates of cancer mortality and incidence by site: I. Application of regional cancer survival model to estimate cancer mortality distribution by site. *BMC Cancer*, **2**, 36.
- Matsumoto H, Wada T, Fukunaga K, et al (2004). Bax to Bcl-2 ratio and Ki-67 index are useful predictors of neoadjuvant chemoradiation therapy in bladder cancer. *Jpn J Clin Oncol*, **34**, 124-30.
- Mitra S, Banerjee S, Misra C, et al (2007). Interplay between human papilloma virus infection and p53 gene alterations in head and neck squamous cell carcinoma of an Indian patient population. *J Clin Pathol*, **60**, 1040-7.
- Pal D, Sur S, Mandal S, et al (2012). Prevention of liver carcinogenesis by amarogentin through modulation of G1/S cell cycle check point and induction of apoptosis. *Carcinogenesis*, **33**, 2424-31.
- Sabbir MG, Dasgupta S, Roy A, et al (2006). Genetic alterations (amplification and rearrangement) of D-type cyclins loci in head and neck squamous cell carcinoma of Indian patients: prognostic significance and clinical implications. *Diagn Mol Pathol*, **15**, 7-16.
- Sankaranarayanan R (1990). Oral cancer in India: an epidemiologic and clinical review. *Oral surg, oral med, oral pathol*, **69**, 325-30.
- Slaughter DP, Southwick HW, Smejkal W (1953). Field cancerization in oral stratified squamous epithelium; clinical implications of multicentric origin. *Cancer*, **6**, 963-8.
- Sultana H, Kigawa J, Kanamori Y, et al (2003). Chemosensitivity and p53-Bax pathway-mediated apoptosis in patients with uterine cervical cancer. *Ann Oncol*, **14**, 214-9.
- Tiezzi DG, De Andrade JM, Candido dos Reis FJ, et al (2006). Apoptosis induced by neoadjuvant chemotherapy in breast cancer. *Pathol*, **38**, 21-7.
- Tripathi A, Dasgupta S, Roy A, et al (2003). Sequential deletions in both arms of chromosome 9 are associated with the development of head and neck squamous cell carcinoma in Indian patients. *J Exp Clin Cancer Res*, **22**, 289-97.